

## Convective Cooling on a Heat Sink with a Cross Flow Synthetic Jet

Harinaldi\*, Arief Randy, Aldy Andika, Damora Rhakasywi

<sup>1</sup>Department of Mechanical Engineering, University of Indonesia, Depok, Indonesia

**Abstract:** Miniaturization of electronic products causes the need for a new cooling system that has high thermal efficiency and low energy consumption. Synthetic jet which is based on zero net mass input but non zero momentum is a new approach utilized for cooling system. This research investigated the forced cooling characterization of a cross flow synthetic jet using a double membrane actuator with two different variations of sinusoidal and square wave and was conducted both in computational as well as also experimental stage. Computational stage was conducted by a commercial CFD software of Fluent® with a turbulence model k- $\omega$  SST and meshing elements quad type pave. The experimental work used a function generator to drive the membranes with the variation of sinusoidal and square wave in three oscillation frequencies i.e 80 Hz, 120 Hz, and 160 Hz at fixed amplitude of 0.002 m/s. The heat flux at the heat sink was maintained at three variations of 10, 25 and 50 W/m<sup>2</sup>. The main purpose of this research was to improve and optimize the process of synthetic jet cooling by suppressing the confinement effect that reduced the cooling effect which occurred in an impinging flow configuration. The results showed significant effect of the reduction of the confinement effect phenomena by using the cross flow synthetic jet.

**Keywords:** synthetic jet, heat transfer, wave excitation, heat flux, vortex.

### 1. Introduction

A common problem that usually occurs in electronic devices today is overheating. If we cannot maintain the heat properly, it will affect the performance of the device and reduces its capability. The improvement in cooling technology is needed, especially for the cooling system in electronic devices. Conventionally, fans and heat sinks are used as heat removal devices. However, fans have limitation in their dimensions, because the fans operate based on electromagnetic principle which requires a minimum space in order to assemble the coil, and also requires high power consumption. However, the requirement of miniaturization of electronic devices is a common thing today. With the smaller dimension but higher performance and ability of electronic devices, heat becomes one of main major problem. A new alternative of cooling method that recently attracts many attention is based on a synthetic jet principle. The device used to generate a synthetic jet which is called a synthetic jet actuator (SJA) usually consists of a thin sized piezoelectric membrane and a relatively small cavity. With the advantages, such as the small form factor, higher efficiency, lower energy consumption compare to the fan, synthetic jet offers the new cooling system in electronic devices. Visually, synthetic jet can be described in Fig.1.

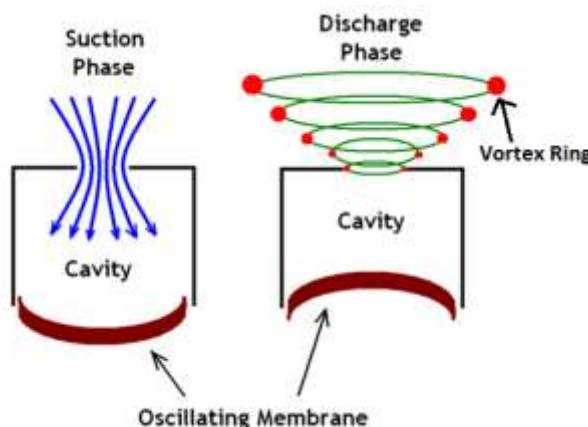


**Figure 1.** Sketch of the synthetic jet formation [3]

Synthetic jet is a fluid flow in the form of a series of vortex rings, which is formed due to the oscillatory movement of the membrane in a cavity [1]. Due to pulsating nature of the flow, the entrainment of ambient fluid into the jet is high as compared to that in a continuous jet, which helps in effective cooling [2]. The vortex that produced by synthetic jet actuator will disturb the laminar flow around the heat source and create a turbulence flow that will increase the cooling process. The synthetic jet formation process has been shown in some work which has been done by Jagannatha et al. [4] and Zhang & Tan [5]. The synthetic jet is formed as follows. Inside the cavity there is a diaphragm or membrane. Membrane will be moved periodically and form a vibration so that the air inside the cavity moves too. The air inside cavity is forced to move through two phases, namely suction and ejection. These two phases are formed due to the orifice on the side of the cavity. At the orifice exit flow separation occurs because of those two phases and forms a vortex ring pair. These vortex rings are used to produce convective heat transfer effect that has better thermal control to the heat sink. The synthetic jet air blower for fuel cell was developed by Choi et.al [6]. The cavity of synthetic jet was made of acrylic with a nozzle for outlet. This synthetic jet was used to flow the hydrogen and oxygen through the cathode and anode in order to create electricity. The synthetic jet was using the excitation of sinusoidal wave and able to generate 500cc/min flow at 650 Hz. Compared to the fuel cell that used fan, this synthetic jet blower was capable of increasing the electricity generated up to 40% Further, and the power consumption of synthetic jet was also relatively small 0.3 W, while the fan consumed 1 W. Overall the synthetic jet blower fuel cell had a better system efficiency than the fan based fuel cell. Lasance et.al [7] studied about the synthetic jet using an asymmetric cavity in purpose to minimize noise and increase cooling efficiency. The objective of the experiments was to get the relations between performance criteria such as the heat transfer coefficient, the dissipated power and the noise and controllable parameters such as pipe dimensions, frequency and voltage. The experiment used pipes with two length for the air outlet 30 and 60 mm and four diameter 3 mm, 4 mm, 5 mm and 6 mm at 3V driving voltage. The result showed that the cavity area such as the pipe length affected the heat transfer characteristic and also the energy consumption of the synthetic jet. Synthetic jet is continuously developed because it has advantages over conventional cooling systems such as fan. For fan system, the need of air supply is filled by flowing the air from one place to another. Synthetic jet system offers major advantages which only use the same air that continuously moving by the system [8]. Mahalingam et al. [9] also considered fan was less efficient by referring to the amount of heat removed per unit volume of flow. Lasance et.al [10] also states another advantages of using synthetic jet cooling system compared with fans for the same heat transfer performance which include lower noise level, much better (thermodynamic) efficiency, half or less power consumption, a better form factor, higher reliability, etc.

Synthetic jet is divided into two models, impinging jet [11] and cross-flow jet [9]. In the present work a comprehensive study was done in both computational and experimental method on an original design of synthetic jet actuators that operate based on membrane made of piezo material to move the air with the vibrations that occur in this membrane. The main focus of the study was to characterize the convective heat transfer of a cross flow configuration in a more realistic condition for an application of cooling an electronic device.

## 2. Method

### 2.1 Computational Work

In this research, computational stage was conducted in order to get a picture of the flow and thermal fields on the cross flow synthetic jet configuration. The work was conducted by using GAMBIT 2.4 software to generate the grid as shown in Fig. 2 and FLUENT 6.3 for the computational solver. The computational model was derived from an originally designed synthetic jet actuator configuration along with the heat sink as the heated wall.

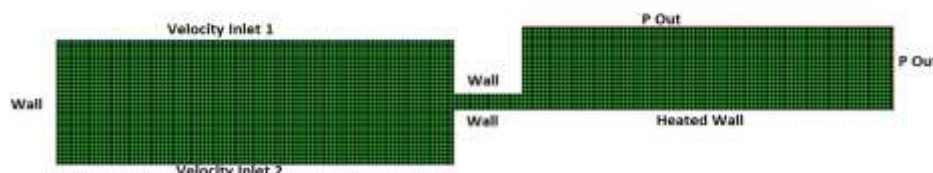


**Figure 2.** Cross flow synthetic jet computational domain

The computational model used to analyze the thermal flow at synthetic jet adopted mathematical model of  $k-\omega$  SST (Shear Stress Transport). The model used 2D Double Precision mode. The SST  $k-\omega$  model is similar to the standard  $k-\omega$  model, but includes the following refinements: (i) the standard  $k-\omega$  model and the transformed  $k-\varepsilon$  model are both multiplied by a blending function and both models are added together. The blending function is designed to be one in the near-wall region, which activates the standard  $k-\omega$  model, and zero away from the surface, which activates the transformed  $k-\varepsilon$  model, (ii) the SST model incorporates a damped cross-diffusion derivative term in the  $\omega$  equation, (iii) the definition of the turbulent viscosity is modified to account for the transport of the turbulent shear stress and (iv) the modeling constants are different.

The SST  $k-\omega$  model has a similar form to the standard  $k-\omega$  model as expressed in equations (1) and (2).

$$\frac{\partial}{\partial t}(\rho k) + \frac{\partial}{\partial x_i}(\rho k u_i) = \frac{\partial}{\partial x_j} \left( \Gamma_k \frac{\partial k}{\partial x_j} \right) + \tilde{G}_k - Y_k + S_k \quad (1)$$

$$\frac{\partial}{\partial t}(\rho \omega) + \frac{\partial}{\partial x_i}(\rho \omega u_i) = \frac{\partial}{\partial x_j} \left( \Gamma_\omega \frac{\partial \omega}{\partial x_j} \right) + G_\omega - Y_\omega + D_\omega + S_\omega \quad (2)$$

The parameters used at this simulation include the model arrangement, the fluid properties and the boundary conditions. Ambient temperature was assumed 27 °C and the heat flux from the bottom of heated wall was maintained at 10, 25 and 50 W/m<sup>2</sup>. Boundary walls on both sides of the actuator assumed to have a constant static pressure with a pressure of 1 atm. Other details of computational conditions are written in Table 1.

Table 1. Computation Condition

Computation Condition		
Model Settings		2D, Unsteady
Fluid		Air
Fluid Properties	Density	1.225 kg/m <sup>3</sup>
	Viscosity	1.7894 e <sup>-5</sup> kg/m-s
	Specific Heat	1006.43 J/kg-K
	Thermal Conductivity	0.0242 W/m-K
Boundary Condition	Velocity Inlet 1,2	UDF
	Pressure Outlet (Gauge Pressure)	0 Pascal
	Heat source	10, 25 and 50 W/m <sup>2</sup>
	Frequency Excitation	80 Hz, 120 Hz and 160 Hz
	Excitation Amplitude	1 m/s

Furthermore, the movement of the diaphragm was modeled with a user defined function (UDF). In this model, at the beginning ( $t = 0$ ), the position of the diaphragm was at the bottom of the cavity. The diaphragm movement was assumed equal to the movement of the piston in a cylinder. The upper membrane was oscillated with sinusoidal wave, which the velocity function is expressed below:

$$V = V_0 + A \sin(2\pi f)t \quad (3)$$

Meanwhile the bottom membrane was oscillated with a square wave, which the velocity function is expressed below:

$$V = V_0 + \frac{A}{\pi} \sum_{n=1,3,5,\dots}^{\infty} \frac{1}{n} \sin(n\pi f)t \quad (4)$$

where A is the maximum speed which was formed due to the movement of the diaphragm inside the cavity, t is the time of experiment and  $V_0$  is the initial velocity .

## 2.2 Experimental Work

Experiment stage was conducted to obtain temperature data of a heat sink which was cooled by the synthetic jet. Experimental setup of the present study is described in Fig. 3. Data was collected by measuring the temperature of the heat sink at four points as described in Fig. 4 by using data acquisition module (Advantech 4718) with an accuracy of measurement  $\pm 0.01$  °C. Heat source at the heat sink was obtained by placing the heater mat at the bottom of the heat sink with a heater mat set at constant flux of 10, 25 and 50 W/m<sup>2</sup> and measurements was performed at ambient temperature of 27 °C and ambient humidity is 70% - 84%. Furthermore, a two-channel function generator was used to excite sinusoidal and square wave signals to upper and lower membrane with excitation of sinusoidal and square wave respectively. The temperature data were picked by thermocouples at 4 points on the heat sink through the DAQ which connected with a computer. Data retrieval in this experiment was carried out for 1 hour at data rate of 1 Hz.

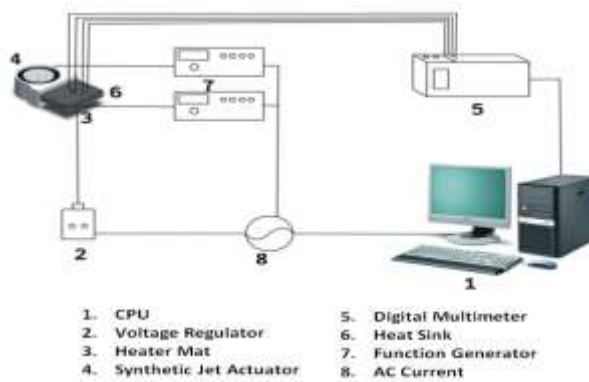


**Figure 3.** Experimental Set-up For Heat Flux Constant Condition

The data of temperature were collected by measuring the temperature at 4 points in the heat sink. As seen in the Fig.13.

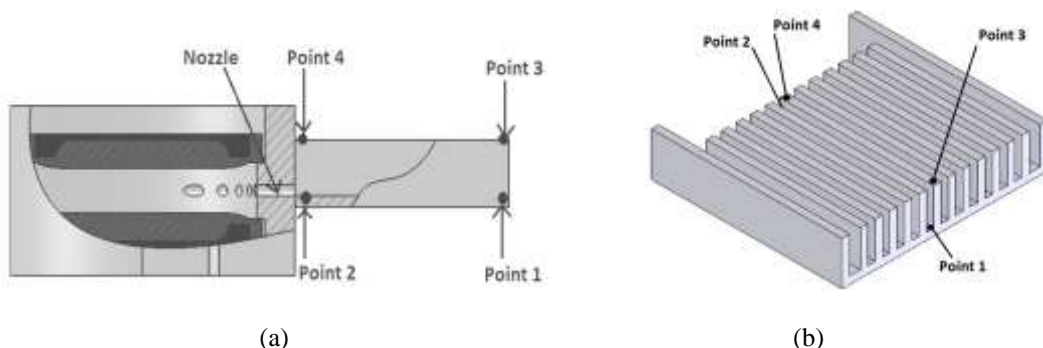


**Fig. 4** Experimental condition (a) Thermocouple placement in the heat sink attach to the actuator (b) Point of temperature measurement in heat sink isometric view

The thermocouples were placed at 4 points in the heat sink. Point 1, 2, 3, and 4. Two thermocouples placed at the bottom of the heat sink, thermocouple 1 at the end of the heat sink and thermocouple 2 near the nozzle. Meanwhile, the thermocouple 1 and 3 were placed at the top of the fin of the heat sink.

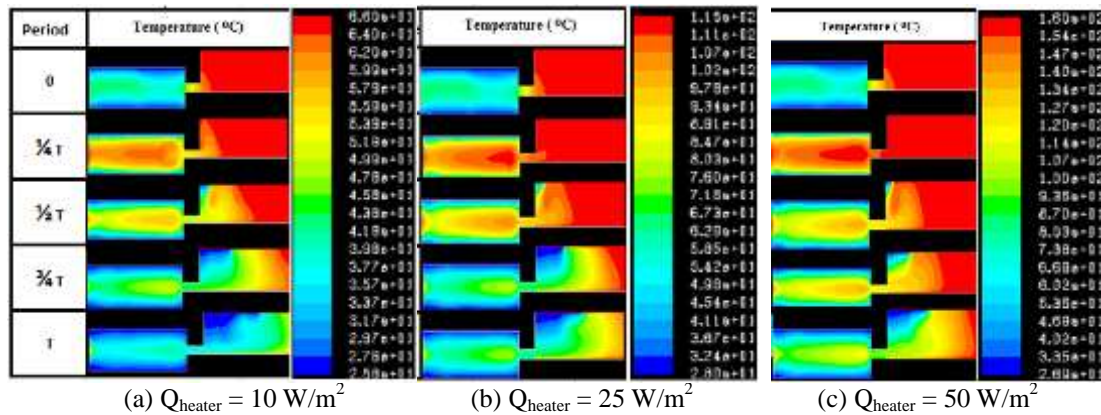
## 3. Results and Discussion

### 3.1 Computational Results

Computational stage is done by analyzing the temperature, velocity, and turbulence intensity contour by performing the flow simulations for 9 combinations of excitation frequencies of upper and lower membrane namely (i) sin 80 Hz-square 80 Hz, (ii) sin 80 Hz-square 120 Hz, (iii) sin 80 Hz-square 160

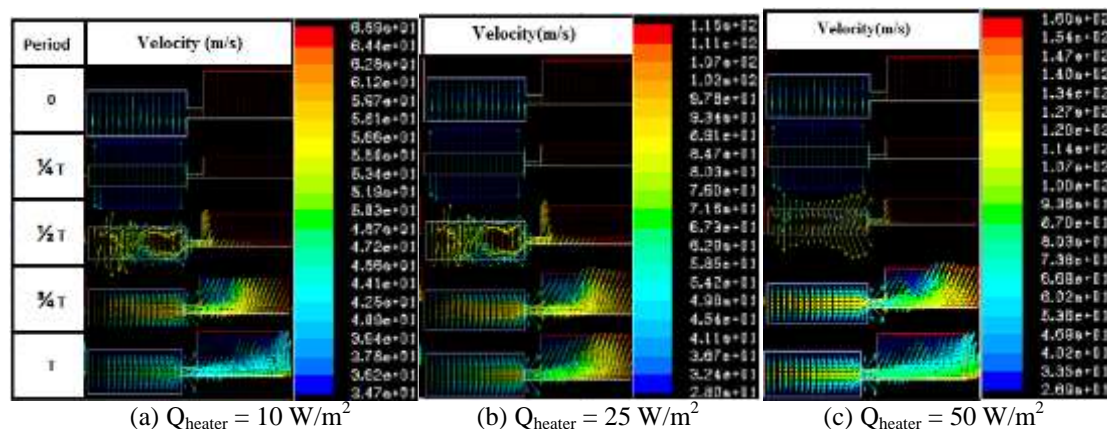
Hz, (iv) sin 120 Hz-square 80 Hz, (v) sin 120 Hz-square 120 Hz, (vi) sin 120 Hz-square 160 Hz, (vii) sin 160 Hz-square 80 Hz, (viii) sin 160 Hz-square 120 Hz, and (ix) sin 160 Hz-square 160 Hz. In the following paragraph only the result of the excitation combination (iv) with sinusoidal 120 Hz at upper membrane and square 80 Hz at lower membrane will be discussed since this combination of excitation produced the best heat transfer rate and hence the optimum cooling effect was obtained.

Fig. 5(a)-(c) shows the temperature contour obtained for the condition of heated wall at 10, 25 and 50  $\text{W/m}^2$  respectively. Series of pictures in Fig. 5 show the change of temperature during the process of cooling by the synthetic jet.



**Figure 5.** Temperature contour with constant heat flux at (a)  $10 \text{ W/m}^2$ , (b)  $25 \text{ W/m}^2$ , (c)  $50 \text{ W/m}^2$

It can be seen that after a quarter of the cycle, the low temperature air starts to flow from the nozzle of synthetic jet actuator and extends to the heat sink to create the cooling process. When the phase has reached the half of the cycle, the cooling effect continues and spread throughout the heat sink until one full wave. This cooling effect will continue until a stagnant condition in which the temperature difference between ambient and around synthetic jet actuator is almost equal and the cooling effect is no longer effective. This stagnant condition, where the accumulation of hot air in the cavity happened, is called as confinement effect. Further observation indicated that the effect of confinement effect in cross flow jet is not as much as occurred in impinging jet type [12].



**Figure 6.** Velocity field with constant heat flux at (a)  $10 \text{ W/m}^2$ , (b)  $25 \text{ W/m}^2$ , (c)  $50 \text{ W/m}^2$

In Fig. 6 (a)-(c) series of velocity vector plots indicate the dynamics of the flow field during a cycle of synthetic jet operation. A significant increase of the velocity of the air flow from the synthetic jet cavity towards the heat sink through the nozzle can be seen in the first quarter of the cycle. The movement of fluid then propagates into heat sink continuously with the increase of velocity. At the third quarter of the cycle the movement of the air flow has arrived at the side of the heat sink evenly and after a complete cycle the flow of low temperature air rises to all side of the heat sink. This flow field dynamic indicates that synthetic jet flow will be more effective for cooling after a certain time period since the

synthetic jet flow was initiated

### 3.2 Experimental Results

By considering the natural convection effect, the heat energy balance can be evaluated as follow :

$$Q_{i,h} = Q_{o,sj} + Q_{o,nc} \quad (5)$$

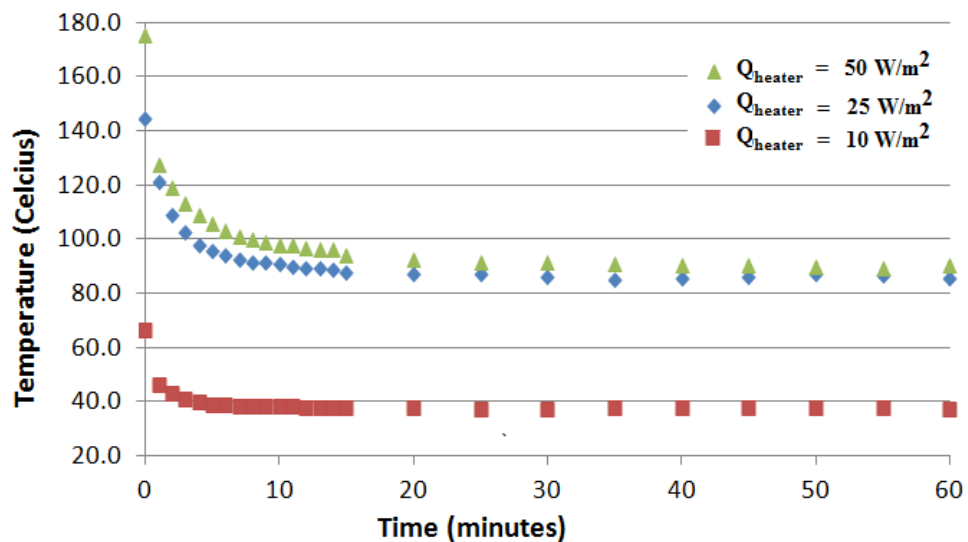
Where  $Q_{i,h}$  is the heat generated by the heater that is conducted through the heat sink,  $Q_{o,sj}$  is the heat removed by the synthetic jet effect, and  $Q_{o,nc}$  is the heat removed by natural convection effect.

The heat transfer coefficient of the synthetic jet  $h_{sj}$  can be evaluated as follow:

$$h_{sj} A_{sj} \left( \frac{dT}{dt} \right) = Q_{i,h} - h_{nc} A_{nc} \left( \frac{dT}{dt} \right) \quad (6)$$

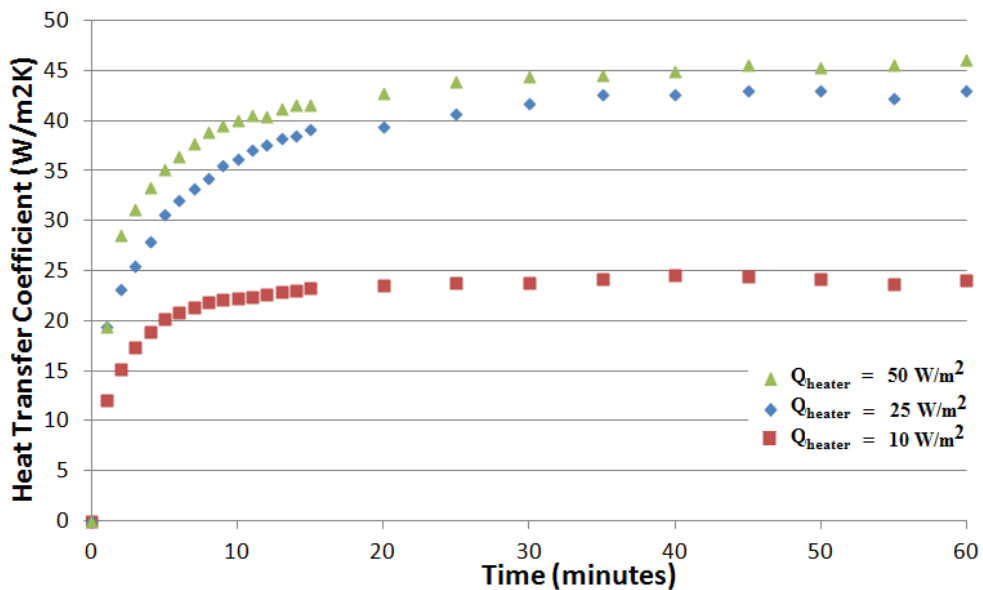
Where  $A_{sj}$  is the synjet effective cooling area,  $(dT/dt)$  is the rate of temperature change measured in the experiment,  $h_{nc}$  is the value of the air heat transfer coefficient with the custom heatsink, and  $A_{nc}$  is the cooling area affected by the air natural convection.

Fig. 7 describes the history of temperature in every constant flux during the cooling period of 60 minutes. It is observable that a rapid decrease of heat sink temperature takes place from the beginning of cooling process until the minimum temperature is achieved and then the temperature slightly rebound to increase. Closer look reveals that the synthetic jet cooling make the temperature decrease ( $\Delta T$ ) up to 29, 55 and 85°C at the heat flux constant of 10, 25 and 50 W/m<sup>2</sup> respectively. Moreover, the effective cooling process occurs at the first 15 – 20 minutes after the synthetic jet actuator generated. After that, the value will change slowly and remain constant until the end of 60 minutes.



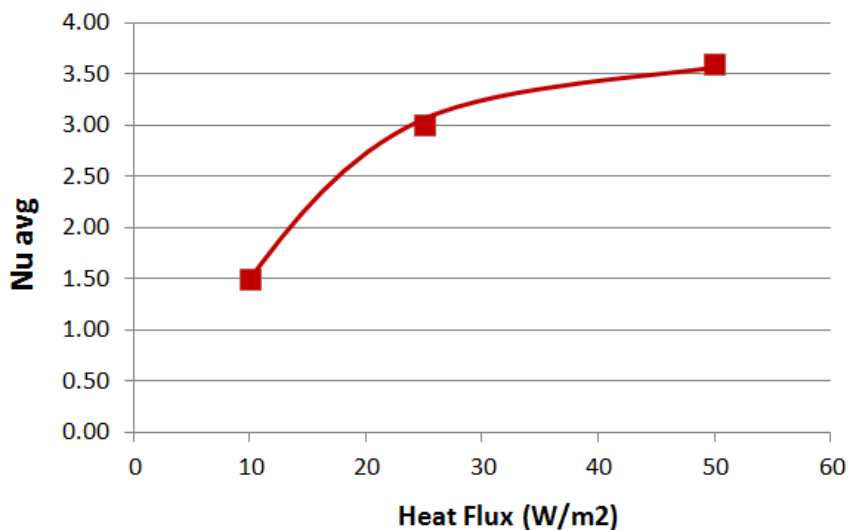
**Figure 7.** Temperature history of heat sink cooled by the synthetic jet

Fig. 8 describes the heat transfer coefficient during the synthetic jet cooling for every condition of heat flux obtained by using the equations (5) and (6).



**Figure 8.** Heat transfer coefficient during the synthetic jet cooling

The heat transfer coefficients over 60 minutes of measurement show similar trend of change since the synthetic jet start to operate for all condition of heat flux given by the heater mat to the heat sink. The graph reconfirms that the effective cooling process occurs at the first 15 to 20 minutes after the synthetic jet actuator generated with the steep increase of heat transfer coefficient within about the first 6 minutes.. After that, the value will change slowly and remain constant until the end of 60 minutes. Furthermore the relation between the heat flux given and the average Nusselt number of cooling process is presented at Fig. 9.



**Figure 9.** Heat Flux vs Average Nusselt

#### 4. Conclusion

The computational and experimental investigation on the convective cooling focussing on the flow and heat transfer characteristics of original designed synthetic jet prototypes has been conducted in a cross flow configuration. The synthetic jet working under the combination of sinusoidal 120 Hz and square 80 Hz with constant flux of 10 W/m<sup>2</sup>, 25 W/m<sup>2</sup>, and 50 W/m<sup>2</sup>. The result shows that the cross flow jet configuration supports the suppression of confinement effect so that it occurs not as much as in impinging jet type. Moreover, the effective cooling process occurs at the first 15 – 20 minutes after the synthetic jet actuator generated with the steep increase of rate of cooling within about first 6 minutes since the synthetic jet was introduced.

## 5. References

- [1]. Smith B.L, Glezer A. The Formation and Evolution of Synthetic Jets. *Physics of Fluid*. 1998; 10: 2281-2297
- [2]. Chaudhari M, Puranik B, Agrawal A. Heat transfer characteristics of synthetic jet impingement cooling, *International Journal of Heat and Mass Transfer*. 2009;11:005
- [3]. Krishnan G., Mohseni K. An Experimental Study of A Radial Wall Jet Formed by the Normal Impingement of A Round Synthetic Jet." *European Journal of Mechanics B/Fluids*. 2010; 29: 269-277
- [4]. Jagannatha D, Narayanaswamy R., and Chandratilleke T.T. Performance Characteristics of A Synthetic Jet Module For Electronic Cooling. *The 10th Heat Transfer Conference in International Symposium On phase Change*. UK. 2007: 8 – 9
- [5]. Zhang J.Z, and Tan X.M. Experimental study on flow and heat transfer characteristics of synthetic jet driven by piezoelectric actuator. *Science in China Series E: Technological Sciences*. 2007; 50: 221-229
- [6]. Sharma R.N. Some insights into synthetic jet actuation from analytical modelling. *The 16th Auatralasian Fluid Mechanics Conference*. 2007 : 1248
- [7]. Mahalingam R, Heffington S, Lee J, and Schwickert M. Newisys server processor cooling augmentation using synthetic jet ejectors. *IEEE*. 2006: 705-709.
- [8]. Lasance C.J.M. and Aarts R.M. Synthetic jet cooling part I: Overview of heat transfer and acoustics. *The 24th IEEE SEMI-THERM Symposium*. 2008 : 20
- [9]. Persoons T, O'Donovan T.S, Murray, D B.. Improving the measurement accuracy of PIV in a synthetic jet flow. *14<sup>th</sup> International Symposium on Applications of Laser Techniques to Fluid Mechanics*. Portugal. 2008
- [10]. McGuinn A, Persoons T, Valiorgue P, O'Donovan T S, and Murray, D B. Heat transfer measurements of an impinging synthetic air jet with constant stroke length. *5<sup>th</sup> European Thermal-Sciences Conference*,Netherlands. 2008 : 6 – 8
- [11]. King S J C, Jagannatha D. Simulation of synthetic jets with non-sinusoidal forcing for heat transfer applications. *18<sup>th</sup> World IMACS / MODSIM Gongress*. Australia.2009 : 1736 – 1737
- [12]. Harinaldi, Damora R, Rikko D. The Effect of Oscillation Mode To The Temperature Distribution of a Heated Wall Impinged by a Synthetic Jet. *The International Conference On QiR (Quality in Research)*. 2011.

## Acknowledgement

This work was supported within the DRPM-UI program of the University of Indonesia (project number 1927/H2.R12.2.1/HKP.05.00/2012).